Available online at www.sciencedirect.com
SCIENCE DIRECT
Journal of Catalysis 241 (2006) 456–464
JOURNAL OF CATALYSIS
www.elsevier.com/locate/jcat

Study of active species of Cu-K/ZrO_2 catalysts involved in the oxidation of soot

H. Laversin, D. Courcot *, E.A. Zhilinskaya, R. Cousin, A. Aboukaïs

Laboratoire de Catalyse et Environnement, E.A. 2598, Université du Littoral – Côte d'Opale, 145, avenue M. Schumann, 59140 Dunkerque, France

Received 6 February 2006; revised 4 May 2006; accepted 8 May 2006

Available online 21 June 2006

Abstract

The effect of the deposition of Cu and K elements on zirconia was studied in the oxidation of a carbon black (CB), considered as a model of diesel soot. Catalytic tests were carried out using CB–catalyst mixtures prepared under loose and tight contact conditions. The potassium-containing catalysts exhibited high activity in loose contact that differed slightly from that obtained in tight contact. The introduction of both Cu and K on ZrO_2 provided synergistic effects in the CB oxidation. It is proposed that these systems can release active oxygen species to oxidize CB even in the absence of gaseous oxygen. Consequently, (CB–catalyst) loose contact mixtures treated at different temperatures under Ar flow were characterized by electron paramagnetic resonance and temperature-programmed reduction measurements. The presence of potassium favours contact between the catalyst and CB and enhances the catalyst's ability to release active oxygen species. In K/ZrO_2, it yields an increase in the amount of Zr^{3+} ions, which appear to be stabilized mainly in monoclinic ZrO_2. In Cu-K/ZrO_2 catalysts, the potassium promoter preferentially interacts with the supported copper(II) species and favours their participation following a redox mechanism.

Keywords: Soot oxidation; Oxide catalysts; Zirconia; Potassium promoter; TPR; EPR

1. Introduction

The development of technologies to achieve reduced particulate emissions from diesel engines remains a subject of interest for the automotive industry, catalyst manufacters, and university laboratories [1,2]. Therefore, the use of a suitable catalyst to enable complete oxidation of soot is considered a promising area of research. Various salts and mixed compounds, including Cu–K–Mo–Cl, Cu–K–V, Cu–K–V–Cl, and $K_{0.7}Cu_{0.3}VO_3 + KCl$, appear to be highly active for soot oxidation considering soot–catalyst mixtures obtained from a "loose contact" preparation method [3–5]. This activity has been explained by the formation of low eutectics that melt at the operating temperature and subsequently increase contact between the active phase and the carbon particles. However, the stability of such catalytic systems is poor, because vapours of active components can be released from the catalyst in operating conditions.

Recently, new investigations have focused on the properties of some metal oxides and mixed metal oxides and their behaviour in the oxidation of carbon black (CB) particles. Despite having lower activity than some salts, metal oxides generally are more stable than salts. Furthermore, the ability of metal oxide to release active oxygen can provide a possible route of investigation for the development of soot oxidation catalysts [6]. The well-known oxygen storage capacity of CeO_2 is a typical example of this. Moreover, the improvement of catalyst preparation methods, the deposition of active phases, and the use of promoters can be expected to enhance the participation of active catalyst species at sufficiently low temperature ranges required in applications.

The aim of this work was to study the catalytic properties of zirconia-supported copper catalysts and the effect of adding potassium as a promoter. Cu_x-K_y/ZrO_2 systems with low copper and/or potassium content ($\leqslant$4 wt% as eq. oxide) were prepared to maintain strong interactions between the ZrO_2 carrier and the supported species, which can be considered as

* Corresponding author. Fax: +33 3 28 65 82 39.
E-mail address: courcot@univ-littoral.fr (D. Courcot).

0021-9517/$ – see front matter
doi:10.1016/j.jcat.2006.05.006

favourable conditions for thermal catalyst stability. The activity of Cu_x-K_y/ZrO_2 systems was evaluated in the oxidation of CB under both "tight" and "loose" contact conditions. To identify some of the catalyst active species participating in the oxidation of carbon, a physicochemical characterization using temperature-programmed reduction (TPR) and electron paramagnetic resonance (EPR) was carried out considering the catalysts or (CB–catalyst) loose contact mixtures.

2. Experimental

2.1. Catalyst synthesis

The zirconium oxide carrier was obtained by a precipitation method, adding an ammoniac solution to a $ZrOCl_2$ solution. The precipitate was washed, filtered, and dried at 100 °C overnight. The resulting solid was calcined under a flow of dry air for 4 h at 600 °C. The ZrO_2 solid thus obtained corresponds to a mixture of tetragonal (JCPDS n° 50-1089) and monoclinic (JCPDS n° 37-1484) crystallized phases. The deposition of copper and potassium was performed by co-impregnation of an aqueous solution containing given amounts of $Cu(NO_3)_2$ and $KHCO_3$ onto the calcined ZrO_2. After drying, all solids were calcined for 4 h at 600 °C. The equivalent amounts of CuO or/and K_2O in calcined catalysts were determined by chemical analysis, and their specific surface areas were obtained using the BET method (Table 1).

2.2. Preparation and testing of (CB–catalyst) mixtures

The carbonaceous particulate material used for the tests was CB N330, provided by Degussa. The elementary analysis revealed the following composition, expressed in wt% [C: 97.23; H: 0.73; O: 1.16; N: 0.19; S: 0.45]. In addition, CB has a BET surface area of 80 $m^2\,g^{-1}$. Before the catalytic tests, CB (6 wt%) and catalyst (94 wt%) were simply mixed inside a zirconia ball using a Teflon stirring rod (light mixing), designating a loose contact between CB and the catalyst surface [7]. To obtain another (CB–catalyst) mixture corresponding to tight contact conditions, CB (6 wt%) and catalyst (94 wt%) were mixed in a ball miller for 40 min.

Table 1
Chemical composition and specific surface area of catalyst samples

Catalysts	Cu content (wt%)	K content (wt%)	K/Cu atomic ratio	Specific surface area (m^2/g)
ZrO_2	–	–		65
$Cu_{1.98}/ZrO_2$	1.58	–		27
$Cu_{3.82}/ZrO_2$	3.05	–		30
$K_{1.77}/ZrO_2$	–	1.47		58
$Cu_{1.98}$-$K_{0.84}/ZrO_2$	1.58	0.70	0.72	23
$Cu_{2.08}$-$K_{1.07}/ZrO_2$	1.66	0.89	0.87	18
$Cu_{1.89}$-$K_{2.22}/ZrO_2$	1.51	1.84	1.98	21
$Cu_{1.96}$-$K_{3.45}/ZrO_2$	1.57	2.87	2.97	22
$Cu_{4.02}$-$K_{1.85}/ZrO_2$	3.21	1.54	0.78	29

Catalytic combustion was studied by simultaneous TG-DTA analysis with a NETZSCH STA 409 apparatus. About 25 mg of the CB–catalyst mixture was loaded in an alumina crucible and heated from 25 to 800 °C at a rate of 5 °C min^{-1} in air flow (75 ml min^{-1}). By processing the experimental data, the onset temperature (T_i) and the final temperature (T_f) could be derived from the TG curve, and the T_m value could be detected at the maximum of the DTA peak. The T_m value gives the temperature at which the CB oxidation rate is maximum. To give examples, Fig. 1 shows the TG-DTA curves obtained during oxidation of CB in the presence of $Cu_{1.98}/ZrO_2$ and $Cu_{2.08}$-$K_{1.07}/ZrO_2$. Considering our experimental conditions [analysis of about 25 mg of (6% CB–94% catalyst) mixture], the TG-DTA curves show that the oxidation reaction occurred regularly without any detection of rapid oxidation phenomena ascribable to a thermal runaway reaction [8]. The analysis of combustion products was performed evaluating the $CO/(CO + CO_2)$ molar ratio from a Varian 3600 chromatograph coupled to a thermobalance.

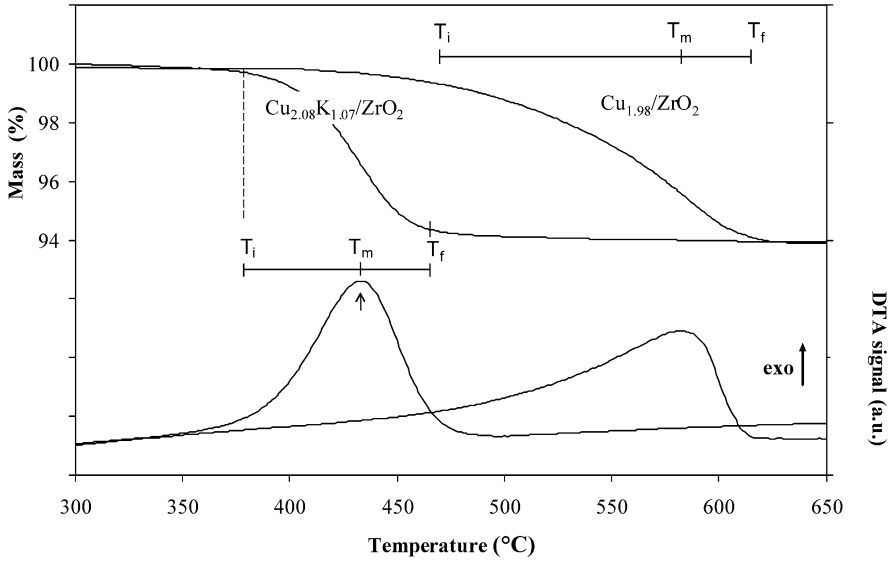

Fig. 1. Examples of TG-DTA measurements for the oxidation of carbon black in the presence of $Cu_{1.98}/ZrO_2$ and $Cu_{2.08}$-$K_{1.07}/ZrO_2$.

2.3. Catalysts and (CB–catalyst) mixture characterization

EPR measurements were performed on a EMX Bruker spectrometer, using a cavity operating at a frequency of ∼9.5 GHz (X-band). The magnetic field was modulated at 100 kHz, and the power supply was sufficiently small to avoid saturation effects. The g values were determined from precise frequency and magnetic field values. Spectra were recorded at ambient temperature and −196 °C, considering the calcined catalysts and the (CB–catalyst) loose contact mixtures treated under Ar at different temperatures. Simulation of experimental spectra was performed using the Bruker SIMFONIA software based on perturbation theory.

The reducibility of the catalysts was determined by H_2-TPR. The experiments were carried out in a conventional apparatus (AMI 200, Zeton Altamira). The catalysts (∼75 mg) were previously treated in situ under O_2 diluted in argon flow at 450 °C for 1 h. After cooling under argon flow, reduction treatment (5% H_2 in argon) was performed with a total flow of 30 mL min^{-1} from 25 °C to 700 °C using a heating rate of 10 °C min^{-1}. Additional experiments involved H_2-TPR measurements of (CB–catalyst) loose contact mixtures previously treated under argon (30 mL min^{-1}) at 400 °C for 1 h. This treatment was considered to simulate the beginning of the CB conversion initiated by the participation of active catalytic species, normally contributing to a redox mechanism. Considering the difference in H_2 consumption for these two kinds of measurements for a given catalyst, information could be obtained on such species reduced by carbon during the Ar treatment at 400 °C.

3. Results and discussion

3.1. Catalytic oxidation of CB

Fig. 2 gives the temperature range in which the oxidation of CB occurred for the test under air of (CB–catalyst) mixtures. Note that the noncatalytic oxidation CB occurred between $T_i = 530$ °C and $T_f = 635$ °C and gave a T_m value of the DTA peak at 615 °C. First, the tests of the loose contact (CB–catalyst) mixtures were undertaken. The results obtained in the presence of ZrO_2 indicated the low reactivity of this oxide carrier. The reaction temperature range for Cu_x/ZrO_2 and ZrO_2 exhibited little difference; the activity increased slightly with increasing Cu content, as indicated by T_i, T_m, and T_f values. The $K_{1.77}/ZrO_2$ catalyst permitted the oxidation reaction to occur between $T_i = 405$ °C and $T_f = 505$ °C, with a maximum oxidation rate at $T_m = 474$ °C. The potassium oxide species lead to significantly improved catalytic activity. As can be seen from Fig. 2, the activity of Cu_x-K_y/ZrO_2 catalysts depends on the Cu and K content. In the case of Cu_x-K_y/ZrO_2 with $x \sim 2$, an important activity increase was obtained up to a K content of $y \sim 1.1$ wt%. The presence of a higher K content induced further slight activity improvement. Note the shift toward lower temperatures of nearly 115 °C on T_i values and 175 °C on T_m values between the tests performed with $Cu_{1.96}$-$K_{3.45}/ZrO_2$ and ZrO_2. Comparing the activity of Cu_x-K_y/ZrO_2 with that

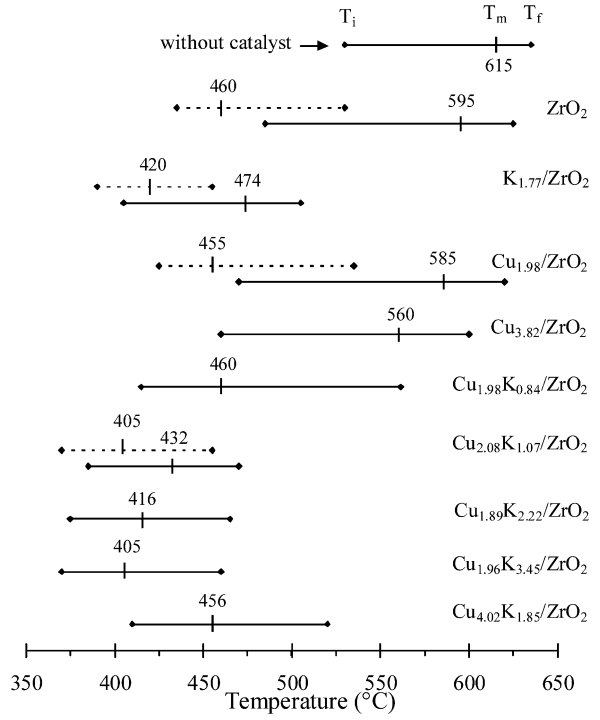

Fig. 2. Temperature ranges of the carbon black oxidation in the presence of Cu_x-K_y/ZrO_2 catalysts. (CB–Cu_x-K_y/ZrO_2) prepared following loose (—) and tight (- - -) contact conditions.

of Cu_x/ZrO_2 and K_y/ZrO_2 with x and $y \sim 2$ reveals synergistic effects related to the addition of both Cu and K on the ZrO_2 surface. Note, however, the decreased catalytic activity in $Cu_{4.02}$-$K_{1.85}/ZrO_2$, probably related to the high proportion of Cu versus K in this solid.

The same dependence of the catalytic activity following the K/Cu ratio in Cu_x–K_{1-x}–O systems was observed by Reichenbach et al. [9]. These authors observed an important decrease in the oxidation onset temperature with increasing K content and then a relative stabilization of this temperature value at higher K content. In our case, however, the more active catalysts were obtained for a higher K/Cu ratio, probably because K and Cu were dispersed on the ZrO_2 carrier. Miro et al. [10] found a similar synergistic effect as in our case between a transition metal and potassium in K-Co/MgO systems. The alkaline metal was found to promote the activity of cobalt oxide species.

Regarding the combustion products, first note that a CO/(CO + CO_2) selectivity of 5–6% was obtained for the combustion of CB performed in the absence of catalyst. Carbon monoxide (CO) was detected in low amounts in the presence of ZrO_2 (∼4%) and Cu/ZrO_2 (∼3%). Moreover, the analysis of combustion products in the presence of all potassium-containing catalysts revealed that only CO_2 was formed. The CO selectivity appeared to be low comparing our data with those of Neeft et al. [11] and Alhström and Odenbrand [12]. However, the CO selectivity in oxidation of soot highly depends on the type of carbonaceous material studied (i.e., diesel soot, synthetic soot, or CB) and the experimental testing conditions. Our results are then found to be in good agreement with the CO selectivity reported for the catalytic oxidation of CB [5,13]. Finally, the

Table 2
EPR parameters values from simulation of experimental spectra and signals assignment[a]

Signal	$g_{//}$	$g_{\perp}$	$A_{//}$	$A_{\perp}$	g_{iso}	ΔH	Assignment
Cu^{2+}(H1)	2.365	2.056	113	16			Highly distorted Cu^{2+} sites (c.n.[b] = 6)
Cu^{2+}(H2)	2.400	2.070	103	15			Highly distorted Cu^{2+} sites (c.n.[b] = 6 or 5)
Cu^{2+}(L)					2.117	300	Cu^{2+} ions in interaction; agglomerated species
S2					2.002	6	Carbonaceous radical in contact with the catalyst surface
Zr^{3+}(T)	1.9590	1.9750					Zr^{3+} in tetragonal ZrO_2
Zr^{3+}(M)	1.9645	1.9735					Zr^{3+} in monoclinic ZrO_2

[a] A and ΔH values given in Gauss.
[b] c.n.: coordination number.

effect of potassium toward a strong decrease in CO selectivity could be partly explained considering that transition metal oxide species promoted by K are also active for CO oxidation [14].

We compared the catalytic behaviour of Cu_x-K_y/ZrO_2 solids following the preparation conditions of the (CB–catalyst) mixtures under "loose" and "tight" contact conditions. The tight contact preparation corresponds to (CB–catalyst) mixtures resulting from ball miller agitation. Corresponding catalytic test results are given by the dashed lines on Fig. 2. In the presence of ZrO_2 and $Cu_{1.98}/ZrO_2$, the conversion of CB occurred in a lower temperature range for the mixtures (CB–catalyst) in tight contact than for the mixtures in loose contact. This indicates that the contact between the CB and the catalyst surface must be created by the physical force obtained from ball milling to obtain a lower reaction temperature. In contrast, for catalysts containing potassium ions ($K_{1.77}/ZrO_2$ and $Cu_{2.08}$-$K_{1.07}/ZrO_2$), the differences in the temperature range for carbon oxidation studied under tight and loose contact conditions are less pronounced. Given this fact, it can be deduced that potassium species promote contact between CB and the catalyst surface.

In summary, the reactivity of Cu_x-K_y/ZrO_2 catalysts in loose contact depends on the copper and potassium content of the solids. For catalysts containing nearly the same copper content (∼2 wt% of eq. CuO), the reactivity of catalysts increases with the potassium content. In contrast, a high proportion of copper versus potassium ($Cu_{4.02}$-$K_{1.85}/ZrO_2$) makes a catalyst less reactive. To gain more insight into the relationship between the catalytic behaviour of Cu_x-K_y/ZrO_2 and Cu and K content, we investigated the physicochemical properties of the catalysts. Our objective was to reveal eventual differences in copper-supported species stabilized in these systems, and in particular, to determine the influence of potassium toward the possible participation of active species of Cu_x-K_y/ZrO_2 catalysts.

3.2. EPR measurements

EPR parameters values from simulation of experimental spectra and signals assignment are presented in Table 2.

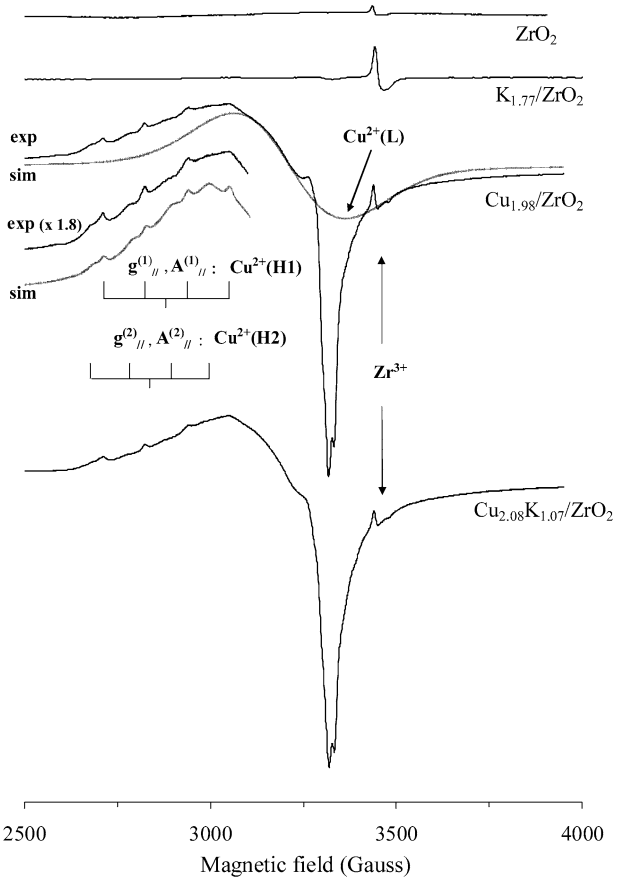

Fig. 3. Experimental and simulated EPR spectra of Cu_x-K_y/ZrO_2 calcined catalysts. (Recording temperature: −196 °C.)

The EPR spectra recorded at −196 °C for the different samples calcined under air at 600 °C are given in Fig. 3. The copper-containing catalysts (Cu_x/ZrO_2 and Cu_xK_y/ZrO_2) give three intense signals with Gaussian shape, denoted as H1, H2, and L, corresponding to Cu^{2+} species. The axial symmetry signals with hyperfine structure are characterized by $g_{//}^{(1)} = 2.365$, $A_{//}^{(1)} = 113$ G, $g_{\perp}^{(1)} = 2.056$, and $A_{\perp}^{(1)} = 16$ G for H1 and by $g_{//}^{(2)} = 2.400$, $A_{//}^{(2)} = 103$ G, $g_{\perp}^{(2)} = 2.070$ and $A_{\perp}^{(2)} = 15$ G for H2. These parameters were determined from simulation of EPR spectra also given in Fig. 3. H1 and H2 signal parameter values are consistent with distorted octahedral Cu(II) entity, characterized by an elongation of the Cu–O bond following the z-axis, in agreement with literature data [15–17]. To state this more precisely, when a (CB–$Cu_{1.98}/ZrO_2$) loose contact mixture was progressively heated under Ar flow at 450 °C, we observed a decrease in H1 intensity but an increase in H2 intensity [18]. When the same mixture was subsequently heated under air flow at 600 °C, CB was completely oxidized, and the intensity ratio between H1 and H2 was restored, as in the case of the initial calcined $Cu_{1.98}/ZrO_2$ catalyst. These observations indicate that Cu^{2+} species giving an H1 signal can be progressively transformed during the treatment described above to give an H2 signal. The subsequent treatment under air demonstrates that this phenomenon is reversible. Species leading to H1 and H2 signals could then occupy the same position in the upper layer of Cu_x-K_y/ZrO_2 solids. The differences in EPR parame-

ters between the H1 and H2 signals can be considered in light of a modification of the Cu(II) site environment. In this way, several authors [15,19–21] have found correlations between $g_{//}$ and $A_{//}$ for different Cu(II) complexes. The evolution of parameters with $g_{//}(\mathrm{H2}) > g_{//}(\mathrm{H1})$ but $A_{//}(\mathrm{H2}) < A_{//}(\mathrm{H1})$ can be related to the increased distortion along the z-axis and/or the enhanced ionic character of the Cu–ligand interaction. In our case, the observation of the reversible phenomenon when the (CB–$Cu_{1.98}/ZrO_2$) mixture was treated under either air or Ar leads us to suggest that the dependence between H1 and H2 is consistent with an increase of the tetragonal distortion of the Cu(II) site up to the loss of one oxygen ligand.

For Cu_x/ZrO_2 and Cu_x-K_y/ZrO_2, L signal ($g_{\mathrm{iso}} = 2.117$, $\Delta H = 300$ G) shown in Fig. 3 can be ascribed to Cu^{2+} ions in interaction, corresponding small agglomerated species [22,23]. The EPR spectra do not indicate differences in the type of Cu^{2+} species depending on the presence or the absence of potassium in the samples. However, comparing H1 and H2 signal intensities reveals that the Cu^{2+} species proportion leading to H2 in comparison to H1 is apparently slightly higher in Cu_x/ZrO_2 than in Cu_x-K_y/ZrO_2. In general, the Cu^{2+} species observed in our case correspond to species dispersed on the ZrO_2 surface (i.e., isolated Cu^{2+} and Cu^{2+} in interaction). But recall that Cu^{2+} species in copper oxide compounds can have antiferromagnetic properties and thus cannot be detected by EPR [24]. A part of Cu^{2+} ions present in the catalysts could not be detected by EPR. For this reason, information on the effect of potassium on Cu(II) species features was investigated using the TPR technique (Section 3.3).

Beside the Cu^{2+} ion EPR signals, the ZrO_2 support gives an axial symmetry signal with g values of $g_{//} < g_{\perp} < g_e = 2.0023$ (Fig. 3) ascribed to Zr^{3+} ions (paramagnetic d^1 ions) [25–29]. The presence of Zr^{3+} ions depends on the occurrence of anionic O^{2-} vacancies [$V(O^{2-})$], because the departure of oxygen species from ZrO_2 is usually described as follows: $O^{2-} \Leftrightarrow 1/2O_2 + V(O^{2-}) + 2e^-$, then $Zr^{4+} + e^- \Leftrightarrow Zr^{3+}$. A more precise assignment of Zr^{3+} signals is given below based on experiments presented in Fig. 4.

The second step of the EPR study was carried out specifically to investigate whether some reducible species could interact with CB, giving an evolution of species that could correspond to paramagnetic species (i.e., Zr^{3+}, Cu^{2+}, radicals). (CB–catalyst) loose contact mixtures were treated under argon flow at different temperatures and studied by EPR. First, the experiments carried out using the less active catalysts (ZrO_2 and Cu_x/ZrO_2) showed a slight reduction of ZrO_2, as deduced from the increased Zr^{3+} signal observed from 400 °C. Our attention was focused on the highly active systems containing the potassium promoter ($K_{1.77}/ZrO_2$ and $Cu_{2.08}$-$K_{1.07}/ZrO_2$).

Fig. 4 shows the EPR spectra recorded at −196 °C for (CB–$K_{1.77}/ZrO_2$) treated at different temperatures under Ar flow. At low temperature (100 °C), the spectrum is similar to that corresponding to the single $K_{1.77}/ZrO_2$ catalyst, which initially gives the Zr^{3+} ion signal with a fivefold-higher intensity than in the case of pure ZrO_2. With an increase in temperature up to 300 °C, a significant increase in Zr^{3+} signal intensity was observed. Furthermore, the corresponding spectrum clearly indicates the superimposition of two signals. To get a high precision on their EPR parameters, this spectrum was simulated (Fig. 5). The two signals, denoted as Zr^{3+}(T) and Zr^{3+}(M), are characterized by $g_{//}(\mathrm{T}) = 1.9590$, $g_{\perp}(\mathrm{T}) = 1.9750$ and $g_{//}(\mathrm{M}) = 1.9645$, $g_{\perp}(\mathrm{M}) = 1.9735$, respectively. Such Zr^{3+} signals were previously reported for ZrO_2. Morterra et al. [28] found that the relative intensity of these signals could vary after the treatment performed on ZrO_2. Matta et al. [29] found a correlation between the signal intensity for these Zr^{3+} ions and the crystallographic phases present in ZrO_2. Indeed, Zr^{3+}(T) and Zr^{3+}(M) signals can be assigned to Zr^{3+} ions in tetragonal and in monoclinic ZrO_2 structures, respectively. At higher temperatures (400 and 500 °C), the Zr^{3+}(M) signal intensity was markedly increased, partly overlapping the Zr^{3+}(T) signal. The increased Zr^{3+} signal intensity can be explained by the reduction of $K_{1.77}/ZrO_2$ surface by carbon. In the absence of potassium, only a slight increase in Zr^{3+}(T) signal intensity occurred in the (CB–ZrO_2) mixture [18]. These observations seem to indicate that potassium species enhanced the reducibility of $K_{1.77}/ZrO_2$ in the presence of carbon, and that higher amounts of Zr^{3+} appeared to be formed on monoclinic ZrO_2 surface crystallites than on tetragonal ZrO_2 ones. Consequently, the potassium promoter could favour the release of oxygen species from the catalyst involving tetragonal and predominantly monoclinic ZrO_2 crystallites.

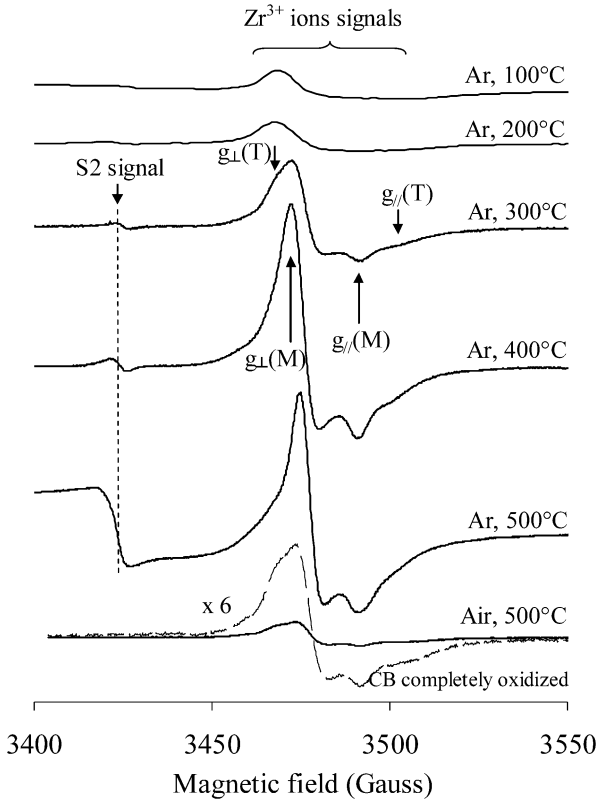

Fig. 4. EPR spectra recorded at −196 °C of (CB–$K_{1.77}/ZrO_2$) loose contact mixture treated at different temperatures under Ar and finally after complete oxidation of carbon black under air at 500 °C.

Finally, the (CB–$K_{1.77}/ZrO_2$) mixture was treated under air flow at 500 °C for 1 h, to ensure the complete oxidation of CB and simulate regeneration of the catalyst. We observed a

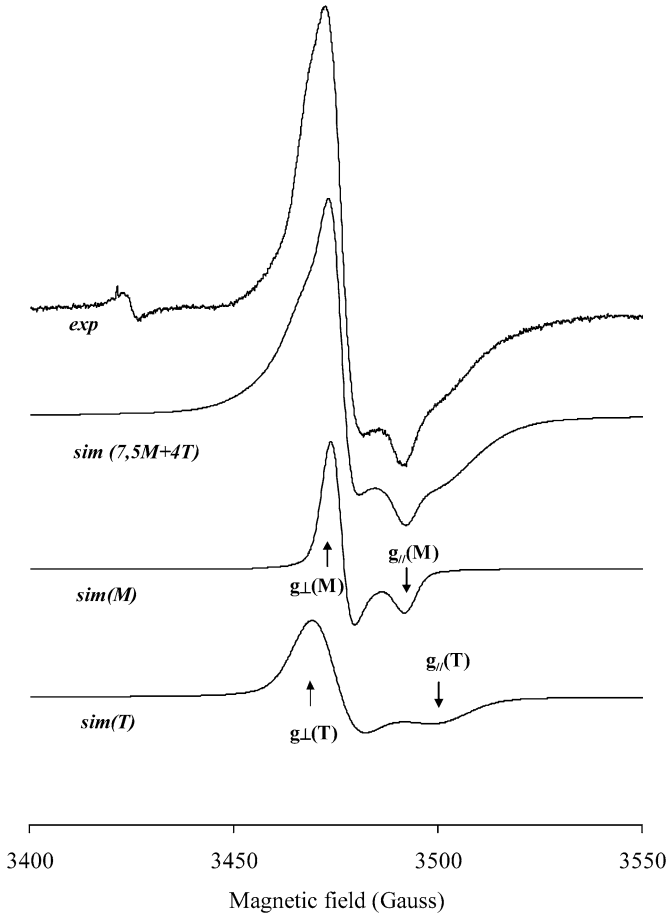

Fig. 5. Experimental and simulated EPR spectrum for Zr^{3+} ions in (CB–$K_{1.77}$/ZrO_2) loose contact mixture treated at 300 °C under Ar. (Recording temperature: −196 °C.)

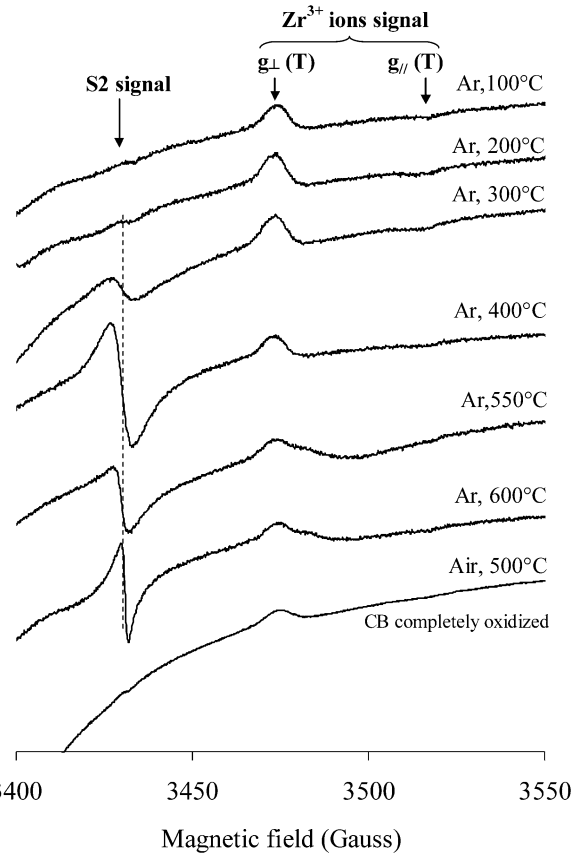

Fig. 6. EPR spectra recorded at −196 °C of (CB–$Cu_{2.08}$-$K_{1.07}$/ZrO_2) loose contact mixture treated at different temperatures under Ar and finally after complete oxidation of carbon black under air at 500 °C.

strong decrease of the Zr^{3+} signal and, in particular, once again more readily differentiated the two Zr^{3+}(T) and Zr^{3+}(M) signals. These findings reveal that the reoxidation of the Zr^{3+} ions occurred, indicating the possible reversibility of the release and uptake of oxygen by the solid.

In parallel, the appearance of a signal designated as S2 ($g = 2.002$ and $\Delta H = 6$ G) occurred only in the presence of K-containing catalysts. According to previous work in our laboratory [30,31], the S2 signal corresponds to carbonaceous radicals formed in CB. More precisely, this signal was observed when CB was in tight contact with the catalyst surface, with this contact created by the physical force of ball milling. This signal was not detected when pure CB was treated in the same temperature range used in this work regardless of atmosphere (air or Ar). It is important to keep in mind that in the present experiments, all CB–catalyst mixtures characterized by EPR and TPR were prepared under loose contact conditions. The S2 signal was observed when the mixture was heated at 300 °C, and its intensity increased at higher temperatures (Fig. 4). In contrast, we did not detect this signal after treating (CB–$Cu_{1.98}$/ZrO_2) and (CB–ZrO_2) mixtures under the same conditions. This means that the S2 signal previously observed only in tight contact appeared in our conditions of loose contact only in the presence of K-containing catalysts, and that the species responsible for the S2 signal could correspond to radicals stabilized at the CB–catalyst interface (exchange layer). This suggests that the S2 signal may reveal the formation of a contact between CB and the K-containing catalyst surface once the mixture is heated from 300 °C.

Note the complete disappearance of the S2 signal due to carbonaceous radicals in contact with the catalyst surface when the (CB–$K_{1.77}$/ZrO_2) mixture was finally treated under air at 500 °C for 1 h. This finding is in agreement with the S2 signal attribution given above, because the complete oxidation of carbon occurred during this treatment.

The EPR spectra obtained for the (CB–$Cu_{2.08}$-$K_{1.07}$/ZrO_2) mixture treated under Ar are displayed in Fig. 6. Whatever the treatment temperature, only the signal of the Zr^{3+} ions in the tetragonal ZrO_2 was detected and no significant evolution of the signal intensity was observed. In comparison with $K_{1.77}$/ZrO_2, it indicates that the presence of copper ions in the catalysts hinders the ZrO_2 reduction. In addition, the S2 signal appeared after treating the mixture at 300 °C and a maximum of intensity was reached after the Ar treatment at 400 °C. The decreased S2 intensity observed over 400 °C is consistent with the oxidation of some CB by the catalyst species able to release the active oxygen species. Quantitative information on the participation of such species, considering the TPR experiments, is given below. The S2 signal was observed only in the presence of K-containing catalysts. The appearance of paramagnetic species

responsible for the S2 signal seems to reflect the formation of the contact between CB and the K-based catalyst surface; such species likely correspond to an intermediate species of the carbon oxidation. This distinctive feature of K_y/ZrO_2 and Cu_x-K_y/ZrO_2 can be correlated to their high activity under loose contact conditions in the oxidation of carbon particulate as described above (Section 3.1).

3.3. TPR measurements

Fig. 7 gives the H_2-TPR profiles obtained for the various catalysts. First, it must be mentioned that no H_2 consumption was recorded for the ZrO_2 support. The support reducibility seems to have been modified in the presence of potassium on ZrO_2, because progressive H_2 consumption was observed from 400 °C on $K_{1.77}/ZrO_2$. More accurate information was deduced in the presence of copper. $Cu_{1.98}/ZrO_2$ showed a single reduction peak at 138 °C, whereas $Cu_{3.82}/ZrO_2$ (with a higher Cu content) exhibited a second reduction component at 210 °C. The most readily reducible species were observed by Shimokawabe et al. [32] and Zhou et al. [33] in calcined systems with nearly the same equivalent CuO content as in our case. The authors ascribed these species to highly dispersed copper(II) species.

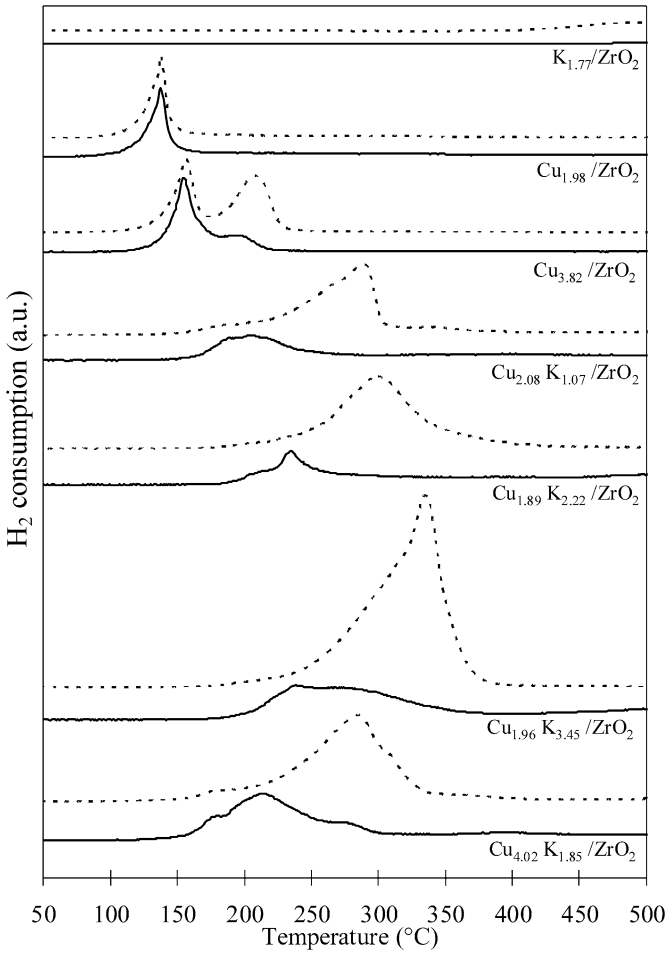

Fig. 7. H_2-TPR profiles obtained for Cu_x-K_y/ZrO_2 catalysts (- - -) and (CB–Cu_x-K_y/ZrO_2) mixtures previously treated under Ar flow (—).

In the case of $Cu_{3.82}/ZrO_2$, assignment of the second reduction peak can be proposed taking into account XRD results (not shown), which demonstrated that CuO crystallites were stabilized in the $Cu_{3.82}/ZrO_2$ catalyst. In fact, the reduction of CuO generally occurred at a temperature close to 350 °C in the H_2-TPR experiments; however, the small size of the particle and/or the interaction of the particle with the carrier surface may explain their reduction at this temperature.

In the case of Cu_x-K_y/ZrO_2, it clearly appeared that the peaks were globally shifted toward a higher temperature range, depending on the Cu and K content. For the same Cu content (∼2 wt% CuO), this shift was increasingly significant with increasing K content. It is suggested that the first reduction peak (at 154–192 °C depending on the K content) can be related to the dispersed Cu(II) species on ZrO_2. The dependence of the Cu(II) reducibility on K content demonstrates the interaction between potassium and copper(II) species, also leading to the main reduction peak between 234 and 337 °C. This phenomenon was described by Shiun Chen et al. [34] as the stabilization of a new phase associating K and Cu.

Regarding H_2 consumption, the values obtained in the Cu_x/ZrO_2 samples were consistent with the reduction of Cu(II) species to Cu^0. In the Cu_x-K_y/ZrO_2 samples, H_2 consumption was markedly higher than that required for copper oxide phase reduction. Hence, it was suggested that the Cu(II) species interact not only with potassium species, but also with the ZrO_2 support, so that the TPR data can be explained by the reduction of both Cu(II) and surfaces species from the support. For the same Cu content (∼2 wt% CuO), H_2 overconsumption increased with K content (Figs. 7 and 8), demonstrating that the potassium species in the presence of copper favoured the reduction of species from the solid. In contrast, however, the sample with a high copper content ($Cu_{4.02}$-$K_{1.85}/ZrO_2$) was characterized by a relatively low H_2 overconsumption due to a stronger interaction of potassium species with Cu(II) than with the entire solid, including both Cu(II) and the ZrO_2 support.

Taking a similar approach as for the EPR experiments, (CB–catalyst) loose contact mixtures were treated under argon flow at different temperatures and studied by H_2-TPR. The contribution to the TPR profiles due to CB treated under Ar was verified to be negligible in the temperature range considered. Assuming that some species detected in the catalyst TPR profiles are active species contributing to a redox mechanism, (CB–catalyst) loose contact mixtures previously treated in-situ under argon at 400 °C were analyzed by TPR (see Section 2). In this case, catalyst species reduced by CB during the Ar treatment could not be reduced during the subsequent H_2-TPR measurement. For solids containing only copper, the peak attributed to dispersed Cu(II) was not modified during the treatment under argon of the (CB–Cu_x/ZrO_2). Although this species was easily reducible under H_2, no reduction occurred in the presence of carbon. This can be explained by the absence of contact between these species and carbon. In contrast, the strong decrease in the peak relative to CuO particles ($Cu_{3.82}/ZrO_2$) reveals the activity of such species in the oxidation of carbon, in good agreement with previous studies [35,36]. For solids containing both potassium and copper, a strong decrease in the TPR

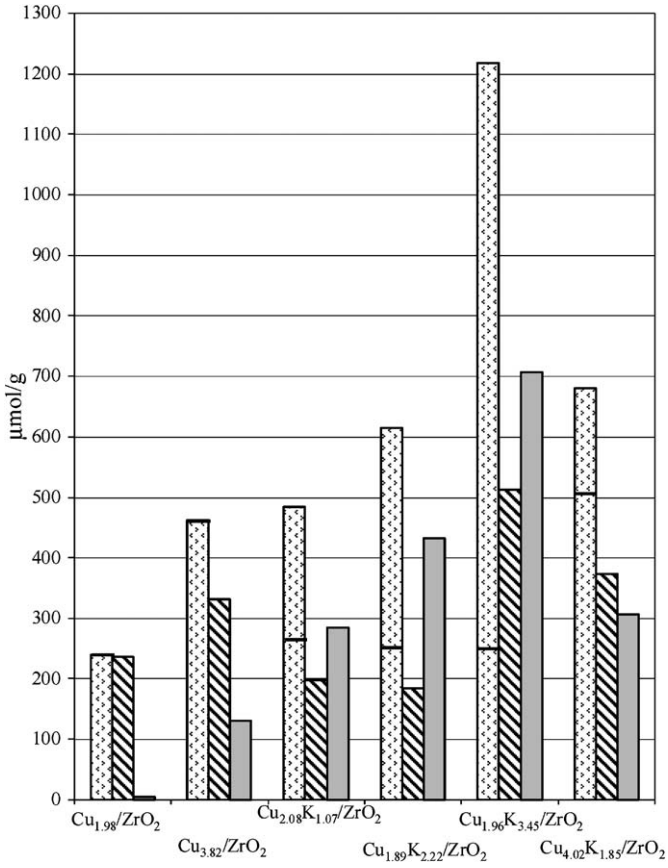

Fig. 8. Quantitative data of TPR experiments on Cu_x-K_y/ZrO_2 catalysts. (▨) Experimental H_2-consumption; the full line in the first column indicates the theoretical H_2-consumption needed for the reduction of eq. CuO into Cu^0. (▧) H_2-consumption obtained after Ar treatment at 400 °C of (CB–catalyst) mixtures. (▩) Calculated oxygen species amount released from the catalyst during the treatment at 400 °C of (CB–catalyst) mixtures.

peak intensity was observed for the catalysts species reduced at 285–337 °C. These species were then reduced by carbon during pre-treatment; this reduction was marked for Cu_x-K_y/ZrO_2 with a high K content. In parallel, catalytic tests performed under Ar indicated the greater conversion of carbon with higher K content in Cu_x-K_y/ZrO_2. Our observations clearly demonstrate that potassium act as a promoter able to enhance the participation of oxygen species from the solid (Fig. 8). Note finally that the remaining TPR peaks probably also include the reduction of surface oxygenated complexes formed on CB during Ar treatment at 400 °C. This phenomenon cannot be excluded and can be explained by the CB–catalyst interaction and oxygen transfer from the Cu_x-K_y/ZrO_2 catalysts.

Note that the reduction peaks obtained after the Ar pretreatment of (CB–catalyst) mixtures were shifted toward low temperatures in comparison with corresponding catalysts. It seems that the treatment under Ar should lead to an evolution of the species resulting from the interaction between copper(II) and potassium species, although the sample preparation included a calcination at 600 °C. The fact that the remaining supported species were more reducible than the fresh catalyst ones could indicate that the Cu(II) species had less interaction with potassium because of the contact of the active phase with carbon. This phenomenon could be related to the mobility of potassium, responsible for the good contact between carbon and the catalyst surface. In this way, for the reaction of K-Mo oxide systems with carbon, Mul et al. [37] showed that a disproportionation K-Mo-O phase might yield on one hand potassium oxide clusters and on the other hand mixed oxide particles with a higher Mo/K ratio. We suggest a similar phenomenon to explain our TPR data on (CB–Cu_x-K_y/ZrO_2).

Our EPR data lead us to propose that ZrO_2 can release lattice oxygen in $K_{1.77}$/ZrO_2 (Fig. 4), but this phenomenon was hindered in Cu_x-K_y/ZrO_2 (see the data for $Cu_{2.08}$-$K_{1.07}$/ZrO_2 in Fig. 6). Nevertheless, the latter system was the most active in CB oxidation (Fig. 2). From the TPR experiments on (CB–catalyst) mixtures, it appears that for Cu_x-K_y/ZrO_2 with low K content, the oxygen species were released mainly from the oxide phase resulting from the interaction between copper(II) and potassium species (Fig. 8). It then can be deduced that the presence of potassium enhances the participation of the copper oxide phase via a redox mechanism. With increasing potassium content (Fig. 8), the amount of oxygen species from the catalysts reacting with CB is greater than that theoretically released, considering the reduction of eq. CuO into Cu^0. This means that both oxygen from copper oxide and lattice oxygen from ZrO_2 can be involved in CB oxidation in Cu_x-K_y/ZrO_2 catalysts with high K content.

Finally, comparing the behaviour of Cu_x/ZrO_2 and Cu_x-K_y/ZrO_2 (Fig. 7) shows that potassium plays a role in improving the redox properties of copper oxide species in the oxidation of soot. Besides ensuring better (CB–catalyst) contact, alkali can favour the transfer of active oxygen species from the copper oxide phase to oxidize carbon. Furthermore, considering the high oxidation rate obtained under air in the presence of Cu_x-K_y/ZrO_2 [7], it can be supposed that the potassium species also facilitate the reoxidation of active copper species involved in the catalytic reaction.

4. Conclusions

Our investigation of the catalytic oxidation of CB on Cu- or/and K-containing ZrO_2 systems has revealed that Cu(II) species supported on ZrO_2 were not sufficiently reactive to provide effective catalysts under loose contact conditions. A significantly decreased CB oxidation temperature range was achieved in the presence of K-containing systems (K/ZrO_2 and Cu-K/ZrO_2). The high activity is related to the contact between CB and the K-containing catalyst surface on heating. This contact is evidenced by the formation of carbonaceous radicals at the CB–catalyst interface. Due to the presence of the potassium promoter even in low amounts, the catalysts are able to release active oxygen species involved in the oxidation of CB. For K/ZrO_2, these species are issued mainly from the oxide support, because K favours the reduction of the monoclinic form of ZrO_2 in the CB oxidation reaction. The K promoter interacts with Cu(II) species in Cu-K/ZrO_2, enhancing the redox properties of the copper oxide phase. Our findings support the role of alkali promoters as species that not only favour CB–catalyst contact,

but also enhance the participation of active oxygen from transition metal oxide and oxide carrier to oxidize soot.

Acknowledgments

The authors are grateful for financial support from the Region Nord-Pas de Calais and the European Community (EDRF).

References

[1] B.A.A.L. van Setten, M. Makkee, J.A. Moulijn, Catal. Rev. 43 (2001) 489.
[2] M. Ambrogio, G. Saracco, V. Specchia, C. van Gulijk, M. Makkee, J.A. Moulijn, Sep. Purif. Technol. 27 (2002) 195.
[3] V. Serra, G. Saracco, C. Badini, V. Specchia, Appl. Catal. B Environ. 11 (1997) 307.
[4] G. Mul, J.P.A. Neeft, F. Kapteijn, M. Makkee, J.A. Moulijn, Appl. Catal. B Environ. 6 (1995) 339.
[5] C. Badini, G. Saracco, V. Serra, V. Specchia, Appl. Catal. B Environ. 18 (1998) 137.
[6] A. Bueno-Lopez, K. Krishna, M. Makkee, J.A. Moulijn, Catal. Lett. 99 (2005) 203.
[7] D. Courcot, C. Pruvost, E.A. Zhilinskaya, A. Aboukaïs, Kinet. Catal. 45 (2004) 614.
[8] J.P.A. Neeft, F. Hoornaert, M. Makkee, J.A. Moulijn, Thermochim. Acta 287 (1996) 261.
[9] H.M. Reichenbach, H. An, P.J. McGinn, Appl. Catal. B Environ. 44 (2003) 347.
[10] E. E Miro, F. Ravelli, M.A. Ulla, L.M. Cornaglia, C.A. Querini, Catal. Today 53 (1999) 631.
[11] J.P.A. Neeft, T. Xander Nijhuis, E. Smakman, M. Makkee, J.A. Moulijn, Fuel 76 (12) (1997) 1129.
[12] A.F. Ahlström, C.U.I. Odenbrand, Carbon 27 (3) (1989) 475.
[13] G. Saracco, N. Russo, M. Ambrogio, C. Badini, V. Specchia, Catal. Today 60 (2000) 33.
[14] C.A. Querini, L.M. Cornaglia, M.A. Ulla, E.E. Miro, Appl. Catal. B Environ. 20 (1999) 165.
[15] L.D. Bogomolova, E.G. Grechko, V.A. Jacchkin, N.A. Krasil'nikova, V.V. Sahkarov, J. Non-Cryst. Solids 86 (1986) 293.
[16] Z. Liu, W. Ji, L. Dong, Y. Chen, J. Catal. 172 (1997) 243.
[17] S.P. Kulyova, E.V. Lunina, V.V. Lunin, B.G. Kostyuk, G.P. Muravyova, A.N. Kharlanov, E.A. Zhilinskaya, A. Aboukaïs, Chem. Mater. 13 (2001) 1491.
[18] D. Courcot, E.A. Zhilinskaya, M. Labaki, H. Laversin, A. Aboukaïs, submitted for publication.
[19] D. Kivelson, R. Neiman, J. Chem. Phys. 33 (1) (1961) 149.
[20] L.D. Bogomolova, Phys. Chem. Glasses 2 (1) (1976) 4.
[21] J. Soria, A. Martinez-Arias, A. Martinez-Chaparro, J.C. Conesa, Z. Schay, J. Catal. 190 (2000) 352.
[22] G.D. Lei, B.J. Adelman, J. Sarkany, W.M.H. Sachtler, Appl. Catal. B Environ. 5 (1995) 245.
[23] C. Pruvost, D. Courcot, E. Abi-Aad, E.A. Zhilinskaya, A. Aboukaïs, J. Chim. Phys. 96 (1999) 1527.
[24] P. A Berger, J.F. Roth, J. Phys. Chem. 71 (1967) 4307.
[25] M.J. Torralvo, M.A. Alario, J. Soria, J. Catal. 86 (1984) 473.
[26] F.R. Chen, G. Coudurier, J.F. Joly, J.C. Vedrine, J. Catal. 143 (1993) 616.
[27] H.W. Liu, L.B. Feng, X.S. Zhang, Q.J. Xue, J. Phys. Chem. 99 (1995) 332.
[28] C. Morterra, E. Giamello, L. Orio, M. Volante, J. Phys. Chem. 94 (1990) 3111.
[29] J. Matta, J.F. Lamonier, E. Abi-Aad, E.A. Zhilinskaya, A. Aboukaïs, Phys. Chem. Chem. Phys. 1 (1999) 4975.
[30] M. Bokova, Ph.D. Thesis, University of Littoral – Côte d'Opale, Dunkerque, France (2004).
[31] E. Saab, M. Bokova, E. Abi-Aad, E.A. Zhilinskaya, A. Aboukaïs, Carbon, in press.
[32] M. Shimokawabe, H. Asakawa, N. Takezawa, Appl. Catal. 59 (1990) 45.
[33] R. Zhou, T. Yu, X. Jiang, F. Chen, X. Zheng, Appl. Surf. Sci. 148 (1999) 263.
[34] C. Shiun Chen, W.H. Cheng, S. Shiun Lin, Appl. Catal. A Gen. 238 (2002) 55.
[35] J.P.A. Neeft, M. Makkee, J.A. Moulijn, Chem. Eng. J. 64 (1996) 295.
[36] C. Pruvost, J.F. Lamonier, D. Courcot, E. Abi-Aad, A. Aboukaïs, Stud. Surf. Sci. Catal. 130 (2000) 2159.
[37] G. Mul, F. Kapteijn, J.A. Moulijn, Carbon 37 (1999) 401.